



Material tailoring for orthotropic elastic rotating disks

G.J. Nie^a, Z. Zhong^{a,*}, R.C. Batra^b

^a School of Aerospace Engineering and Applied Mechanics, Tongji University, Shanghai 200092, China

^b Department of Engineering Science and Mechanics, M/C 0219, Virginia Polytechnic Institute and State University, Blacksburg, VA 24061, USA

ARTICLE INFO

Article history:

Received 26 October 2010

Received in revised form 6 December 2010

Accepted 9 December 2010

Available online 14 December 2010

Keywords:

A. Structural composites

A. Fibers

C. Elastic properties

Material tailoring

ABSTRACT

The tailoring of elastic moduli in the radial direction is studied to design a fiber-reinforced orthotropic linear elastic rotating disk with constant radial or hoop stress or constant in-plane shear stress. For fibers arranged in concentric circles the axes of material symmetry coincide with the radial and the circumferential directions. However, when fibers are aligned along helices, the orientation of material principal axes varies with the radial coordinate of a point. For a solid disk made of an orthotropic material with Young's moduli proportional to each other, we give explicit expressions for the required variations of the elastic moduli with the radius to attain a given state of stress. For a rotating annular disk composed of a fiber-reinforced composite with fibers placed along concentric circles, the required radial variation of the volume fraction of fibers is calculated numerically and exhibited graphically. For fibers of known volume fraction laid along helices, the radial variation of the fiber orientation angle is determined. We have also analyzed the material tailoring problem for a disk of variable thickness. Results presented herein should help structural engineers and material scientists optimally design rotating disks composed of radially inhomogeneous materials.

© 2010 Elsevier Ltd. All rights reserved.

1. Introduction

Direct problems concerned with finding stresses and displacements in a structure of known shape and composed of inhomogeneous materials, such as fiber-reinforced composites and functionally graded materials (FGMs), have been studied extensively [1–10]. Generally an inhomogeneous material has material moduli varying in one or more spatial directions. However, much less efforts have been devoted to the optimization of structural topology and spatial variation of material moduli when a structure is subjected to prescribed loads. For a structure with fixed geometry the optimization problem is reduced to finding the gradation of material properties so as to achieve the desired stress state in the body. Such problems are usually called material tailoring and we address here a rotating disk of variable thickness.

Designing an inhomogeneous, orthotropic and linear elastic structure to yield a desired spatial distribution of stresses has been studied by Leissa and Vagins [11]. Assuming all material moduli proportional to each other, they determined the spatial variation of material moduli to have either the hoop stress or the in-plane shear stress uniform throughout the cylinder thickness and in a rotating disk. Pardoen et al. [12] investigated implications of varying the mass and the stiffness properties in order to achieve a desired stress state in a thick-rim flywheel. Desirable stress states

include having either the hoop stress or the in-plane shear stress uniform in a cylinder, a sphere and a disk. Danfelt et al. [13] optimized the design of a fiber-reinforced multi-ringed composite flywheel by varying the thickness, Poisson's ratio, Young's modulus and the mass density so that each ring will fail at approximately the same angular speed. Adali et al. [14] maximized the rotational speed of composite disks by determining the fiber orientations and the lamination scheme using the Tsai–Wu strength criterion. Gowayed et al. [15] used a sequential quadratic programming approach to optimally design a composite flywheel by varying reinforcements in the hoop and the radial directions. Jain et al. [16] designed a constant thickness composite disk of uniform strength by radially tailoring the elastic moduli, and Güven et al. [17] found the radial variation of elastic moduli to attain uniform radial stress in the disk. Fabien [18] studied the optimal design of a stacked-ply composite flywheel with fibers oriented either in the hoop or in the radial direction. Cho and Rowlands [19] optimized fiber directions to reduce stress concentrations in perforated composites.

Based on optimization techniques and the finite element method (FEM), Tanaka et al. [20–22] determined the spatial variation of the constituent phases of FGMs to minimize thermal stresses. Batra and Jin [23] optimized the natural frequencies of a laminated composite plate by changing the fiber orientation in each ply. Qian and Batra [24] employed a higher-order shear and normal deformable plate theory and a meshless method to compute the spatial variation of the volume fractions of constituents to optimize natural frequencies of a FG cantilever plate. Goupee and Vel [25,26] employed

* Corresponding author.

E-mail address: zhongk@tongji.edu.cn (Z. Zhong).

a genetic algorithm to optimize the spatial distribution of the constituent phases of FGMs. For cylinders and spheres made of incompressible and isotropic Hookean materials, Batra [27] analytically found the radial variation of the shear modulus so that either the hoop stress or the in-plane shear stress is uniform during their axisymmetric deformations. Nie and Batra [28] have determined the radial variation of either Young's modulus or Poisson's ratio for a cylinder to have either uniform in-plane shear stress or uniform hoop stress during axisymmetric deformations; they [29,30] have also analyzed similar problems for incompressible linear elastic materials.

In this paper, we investigate how to tailor material moduli for achieving a desirable stress field in a rotating disk composed of radially inhomogeneous materials. For a disk made of an orthotropic material we find the required radial variation of the elastic moduli. For a disk made of a composite material with fibers arranged in concentric circles we find the radial variation of the volume fraction of fibers, and for fibers oriented in helices we find the radial orientation of fibers.

2. Problem formulation

2.1. Basic equations

Consider a thin circular disk of non-uniform thickness $h(r)$, inner radius r_{in} , outer radius r_{ou} , and rotating at a constant angular velocity, ω , about the centroidal axis perpendicular to the plane of the disk, as shown in Fig. 1. The thickness of this annular disk is assumed to vary as a function of the radius according to the relation

$$h(r) = h_{ou} \left(\frac{r}{r_{ou}} \right)^{-n}, \quad (1)$$

where n ($n \geq 0$) is a constant, and h_{ou} is the thickness of the disk at $r = r_{ou}$. For $n = 0$ the disk thickness is uniform. For a solid disk the thickness is assumed to be uniform. The maximum thickness of the disk is assumed to be sufficiently small as compared to its outer diameter so that the assumption of the plane state of stress is reasonable. We use cylindrical coordinates (r, θ, z) with the origin at the disk center and the z -axis perpendicular to the plane of the disk to describe its deformations.

For a thin rotating disk of variable thickness, in the absence of gravitational forces, the equation of equilibrium in the radial direction is [31]

$$\frac{d}{dr} [h(r)r\sigma_{rr}] - h(r)\sigma_{\theta\theta} + h(r)\rho\omega^2 r^2 = 0, \quad (2)$$

where σ_{rr} and $\sigma_{\theta\theta}$ are, respectively, the radial and the hoop stresses at a point, and ρ is the mass density that is assumed to be a constant. Since the disk thickness varies with r , therefore, the mass density per unit surface area varies with r . Without the assumption of constant ρ we cannot solve the problem since we have more

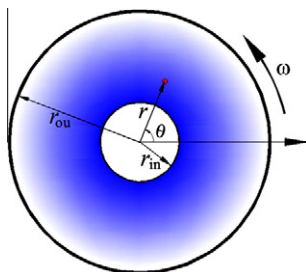


Fig. 1. A rotating disk of variable thickness and composed of an inhomogeneous material.

unknowns than the number of equations. However, if $\rho(r)$ is known, then we should be able to numerically solve the problem. We solve the problem for the following two sets of boundary conditions on the inner and outer surfaces of the disk

(1) Annular disk with its inner and outer surfaces traction free:

$$\sigma_{rr}(r_{in}) = 0.0, \quad \sigma_{rr}(r_{ou}) = 0.0. \quad (3a, b)$$

(2) Solid disk with its outer boundary subjected to normal tractions:

$$\sigma_{rr}(r_{ou}) = \bar{\sigma}_{rr}^{ou}. \quad (3c)$$

Here $\bar{\sigma}_{rr}^{ou}$ is a given value of the normal traction on the outer surface of the disk. Because of the assumption that deformations are axisymmetric, we have

$$u_r(0,0) = 0.0, \quad (3d)$$

where u_r is the radial displacement of a point.

Assuming infinitesimal deformations, the in-plane radial and hoop strains, ε_{rr} and $\varepsilon_{\theta\theta}$, are related to u_r , respectively, by

$$\varepsilon_{rr} = \frac{du_r}{dr}, \quad \varepsilon_{\theta\theta} = \frac{u_r}{r}. \quad (4a, b)$$

The axial strain ε_{zz} in the z -direction is generally non-zero. Eqs. (4a) and (4b) yield the following compatibility equation

$$\frac{d}{dr} (r\varepsilon_{\theta\theta}) - \varepsilon_{rr} = 0. \quad (5)$$

For a disk in a state of plane stress, the pertinent constitutive equations for a radially inhomogeneous polar-orthotropic elastic material with the material principal axes at a point along the radial, the circumferential, and the z -axis are

$$\begin{aligned} \varepsilon_{rr} &= \frac{1}{E_r(r)} (\sigma_{rr} - \nu_{r\theta}(r)\sigma_{\theta\theta}), \\ \varepsilon_{\theta\theta} &= \frac{1}{E_\theta(r)} (-\nu_{\theta r}(r)\sigma_{rr} + \sigma_{\theta\theta}), \end{aligned} \quad (6)$$

where $E_r(r)$ and $E_\theta(r)$ are the elastic moduli in the r and the θ directions, respectively, and $\nu_{r\theta}(r)$ and $\nu_{\theta r}(r)$ are Poisson's ratios satisfying the relation

$$\frac{\nu_{\theta r}}{E_\theta} = \frac{\nu_{r\theta}}{E_r}. \quad (7)$$

2.2. Description of material properties

The macroscopic material parameters of an inhomogeneous body are generally related to its microstructure. Here we consider the following three inhomogeneous materials: (i) polar orthotropic material with the two Young's moduli proportional to each other and the two Poisson's ratios constants; (ii) fiber-reinforced composite with fibers forming concentric circles and the spacing between adjacent fibers a function of r that makes the fiber volume fraction a function of r ; and (iii) fiber-reinforced composite with fibers aligned along helices and slopes β varying with the radius r . The fiber orientations for the last two classes of materials are depicted in Fig. 2.

For a fiber-reinforced composite with fibers aligned along concentric circles and variable spacing between adjacent fibers, elastic moduli of the composite can be expressed in terms of those of the fibers and the matrix and the volume fraction $\xi_f(r)$ of the fibers by [32]

$$\begin{aligned} E_r(r) &= \frac{E_f E_m}{\xi_f(r) E_m + (1 - \xi_f(r)) E_f}, \\ E_\theta(r) &= \xi_f(r) E_f + (1 - \xi_f(r)) E_m, \end{aligned} \quad (8a, b)$$

$$\nu_{\theta r}(r) = \xi_f(r) \nu_f + (1 - \xi_f(r)) \nu_m, \quad \nu_{r\theta}(r) = \frac{E_r(r)}{E_\theta(r)} \nu_{\theta r}(r), \quad (8c-d)$$

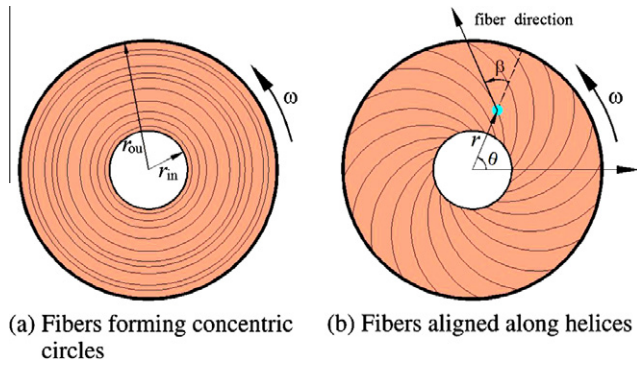


Fig. 2. Two different alignments of fibers in a fiber-reinforced composite rotating disk.

where suffixes m and f denote the matrix and the fiber, respectively. We note that several homogenization techniques have been reported in the literature, e.g., see [33]. The focus of this work is on establishing a methodology for tailoring material properties to attain a desired state of stress in the disk; thus we have used a rather simple homogenization technique.

For fiber-reinforced composites with fibers aligned along helices it is assumed that the radial reinforcement in half of the plies are constructed with the fiber angle of $+\beta(r)$ and the other half with the fiber angle of $-\beta(r)$. Thus the effective compliance matrix for this composite structure corresponds to that of an orthotropic material [18], and the corresponding elastic moduli can be expressed as [34]

$$E_r(r) = \frac{1}{V_1 + V_2 \cos(2\beta(r)) + V_3 \cos(4\beta(r))},$$

$$v_{r\theta}(r) = \frac{-V_4 + V_3 \cos(4\beta(r))}{V_1 + V_2 \cos(2\beta(r)) + V_3 \cos(4\beta(r))}, \quad (9a-c)$$

$$E_\theta(r) = \frac{1}{V_1 - V_2 \cos(2\beta(r)) + V_3 \cos(4\beta(r))},$$

where

$$V_1 = \frac{1}{8} \left(\frac{3}{E_1(r)} + \frac{3}{E_2(r)} - \frac{2v_{12}(r)}{E_1(r)} + \frac{1}{G_{12}(r)} \right),$$

$$V_2 = \frac{1}{2} \left(\frac{1}{E_1(r)} - \frac{1}{E_2(r)} \right),$$

$$V_3 = \frac{1}{8} \left(\frac{1}{E_1(r)} + \frac{1}{E_2(r)} + \frac{2v_{12}(r)}{E_1(r)} - \frac{1}{G_{12}(r)} \right),$$

$$V_4 = \frac{1}{8} \left(\frac{1}{E_1(r)} + \frac{1}{E_2(r)} - \frac{6v_{12}(r)}{E_1(r)} - \frac{1}{G_{12}(r)} \right), \quad (10)$$

and subscripts 1 and 2 denote the fiber and the transverse directions, respectively. $E_1(r)$, $E_2(r)$, $v_{12}(r)$ and $G_{12}(r)$ are determined from Eq. (8) for a given volume fraction of fibers.

3. Desirable stress fields

3.1. Constant hoop stress

Consider the hoop stress to be constant as a desired plane stress state in the disk, that is,

$$\sigma_{\theta\theta} = C_1, \quad (11)$$

where C_1 is related to the boundary conditions.

By simultaneously solving Eqs. (11) and (2) and considering boundary conditions listed in Eq. (3), we find stresses in the disk.

Case 1: Annular disk with the inner and the outer surfaces traction free

For a constant hoop stress throughout the disk, the radial and the hoop stresses, respectively, are given by

$$\sigma_{rr}(r) = \frac{\rho\omega^2(r^n R_1 + r^3 R_2 + r R_3)}{(n-3)R_2 r},$$

$$\sigma_{\theta\theta}(r) = \frac{\rho\omega^2(1-n)R_3}{(n-3)R_2}, \quad \text{for } n \neq 1, n \neq 3, \quad (12a, b)$$

$$\sigma_{rr}(r) = \frac{\rho\omega^2(R_4 \ln r - R_5 r^2 + R_6)}{2R_5},$$

$$\sigma_{\theta\theta}(r) = \frac{\rho\omega^2 R_4}{2R_5}, \quad \text{for } n = 1, \quad (13a, b)$$

$$\sigma_{rr}(r) = \frac{\rho\omega^2(-R_4 r^2 \ln r + R_7 r^2 + R_8)}{R_4},$$

$$\sigma_{\theta\theta}(r) = \frac{2\rho\omega^2 r_{in}^2 r_{ou}^2 R_5}{R_4}, \quad \text{for } n = 3, \quad (14a, b)$$

where $R_1 = r_{in} r_{ou} (r_{in}^2 - r_{ou}^2)$, $R_2 = r_{in} r_{ou}^n - r_{in}^n r_{ou}$, $R_3 = r_{in}^n r_{ou}^3 - r_{in}^3 r_{ou}^n$, $R_4 = r_{in}^2 - r_{ou}^2$, $R_5 = \ln(r_{in}/r_{ou})$, $R_6 = r_{ou}^2 \ln r_{in} - r_{in}^2 \ln r_{ou}$, $R_7 = r_{in}^2 \ln r_{in} - r_{ou}^2 \ln r_{ou}$, $R_8 = r_{in}^2 r_{ou}^2 \ln(r_{ou}/r_{in})$, and the value of n describes the variation of the disk thickness according to Eq. (1).

Case 2: Solid disk with its outer boundary subjected to normal tractions

For a constant hoop stress throughout the solid disk of uniform thickness (i.e., $n = 0$ in Eq. (1)) the radial and the hoop stresses, respectively, are given by

$$\sigma_{rr}(r) = \frac{\rho\omega^2(r_{ou}^2 - r^2)}{3} + \bar{\sigma}_{rr}^{ou}, \quad \sigma_{\theta\theta}(r) = \frac{\rho\omega^2 r_{ou}^2}{3} + \bar{\sigma}_{rr}^{ou}. \quad (15a, b)$$

3.2. Constant in-plane shear stress

Consider the in-plane shear stress to be uniform throughout the disk as a desired stress state,

$$\sigma_{\theta\theta} - \sigma_{rr} = C_2, \quad (16)$$

where C_2 is related to the boundary conditions. For $C_2 = 0$, Eq. (16) implies that the radial and the hoop stresses are equal to each other at every point in the disk; this stress state in an axisymmetric rotating disk has been discussed in [16,17].

Simultaneously solving Eqs. (16) and (2) and considering Eq. (3), we get the following expressions for stresses for the annular and the solid disks.

Case 3: Annular disk with the inner and the outer boundaries traction free

For a constant in-plane shear stress throughout the disk the radial and the hoop stresses are given by

$$\sigma_{rr}(r) = \frac{\rho\omega^2(-r^n R_4 + r^2 R_9 + R_{10})}{(n-2)R_9},$$

$$\sigma_{\theta\theta}(r) = \frac{\rho\omega^2(-r^n R_4 + r^2 R_9 + (1-n)R_{10})}{(n-2)R_9}, \quad \text{for } n \neq 0, n \neq 2 \quad (17a, b)$$

$$\sigma_{rr}(r) = \frac{\rho\omega^2(R_4 \ln r - R_5 r^2 + R_6)}{2R_5},$$

$$\sigma_{\theta\theta}(r) = \frac{\rho\omega^2(R_4(1 + \ln r) - R_5 r^2 + R_6)}{2R_5}, \quad \text{for } n = 0 \quad (18a, b)$$

$$\sigma_{rr}(r) = \frac{\rho\omega^2(-R_4 r^2 \ln r + R_7 r^2 + R_8)}{R_4},$$

$$\sigma_{\theta\theta}(r) = \frac{\rho\omega^2(-R_4 r^2 \ln r + R_7 r^2 - R_8)}{R_4}, \quad \text{for } n = 2 \quad (19a, b)$$

where $R_9 = r_{in}^n - r_{ou}^n$, $R_{10} = r_{in}^2 r_{ou}^n - r_{in}^n r_{ou}^2$.

Comparing Eqs. (13a) and (18a), it is found that expressions for the radial stresses are the same for the disk with constant hoop stress when the thickness is described by Eq. (1) with $n = 1$ and the disk with constant in-plane shear stress when the thickness is uniform ($n = 0$).

Case 4: Solid disk with its outer boundary subjected to normal tractions

In this case the constant C_2 in Eq. (16) must be 0, the in-plane shear stress throughout the disk vanishes, and the radial and the hoop stresses are given by

$$\sigma_{rr}(r) = \sigma_{\theta\theta}(r) = \frac{\rho\omega^2(r_{ou}^2 - r^2)}{2} + \bar{\sigma}_{rr}^{ou}. \quad (20a, b)$$

Expressions for stresses in Eq. (20) are the same as those given in Ref. [16].

3.3. Constant radial stress

We now consider the case of constant radial stress in the disk, that is,

$$\sigma_{rr} = D_0, \quad (21a)$$

where the constant D_0 is related to the boundary conditions. For an annular rotating disk the boundary conditions on the inner and the outer surfaces must be $\sigma_{rr}(r_{in}) = \sigma_{rr}(r_{ou}) = D_0$.

For a solid rotating disk the condition $u_r(0,0) = 0$ is identically satisfied for a constant radial stress state and $\sigma_{rr}(r_{ou}) = D_0$.

Substituting Eq. (21a) and the thickness expression (1) into the equilibrium Eq. (2), the hoop stress is found to be

$$\sigma_{\theta\theta} = D_0(1 - n) + \rho\omega^2 r^2. \quad (21b)$$

Expressions (12)–(21) for stresses are universal for a rotating disk because they are valid irrespective of the material of the disk.

4. Material tailoring for rotating disks

We assume that $E_\theta(r) > 0$, $E_r(r) > 0$ and substitute for strains from the constitutive relation (6) into the compatibility Eq. (5) to arrive at the following first-order ordinary differential equation (ODE) for finding the elastic moduli.

$$\begin{aligned} & \left(\sigma_{\theta\theta} + r \frac{d\sigma_{\theta\theta}}{dr} - \sigma_{rr} v_{\theta r}(r) - r v_{\theta r}(r) \frac{d\sigma_{rr}}{dr} - r \sigma_{rr} \frac{dv_{\theta r}(r)}{dr} \right) E_r(r) \\ & + (r \sigma_{rr} v_{\theta r}(r) - r \sigma_{\theta\theta}) \frac{E_r(r)}{E_\theta(r)} \frac{dE_\theta(r)}{dr} + (\sigma_{\theta\theta} v_{r\theta}(r) - \sigma_{rr}) E_\theta(r) \\ & = 0. \end{aligned} \quad (22)$$

We discuss below the problem of material tailoring in a rotating disk composed of three different inhomogeneous materials described in Section 2.2.

4.1. Solid disk made of a material with Young's moduli proportional to each other

Because there is only one ODE for finding the two elastic moduli and one Poisson's ratio, we employ a simplifying assumption similar to that used by Leissa and Vagins [11] and Bert and Niedenfuhr [35], namely, the two Young's moduli are proportional to each other, and Poisson's ratios are constants. Thus

$$E_r(r) = \alpha E_\theta(r), \quad v_{r\theta} = \alpha v_{\theta r}, \quad (23a, b)$$

where the constant α ($\alpha > 0$) denotes the degree of anisotropy of the material; $\alpha = 1$ for an isotropic material.

Substituting Eq. (23) into Eq. (22), we find its solution to be

$$E_\theta(r) = E_0 \exp \left(\int_{r_{in}}^r g(y) dy \right), \quad (24)$$

where $E_0 = E_\theta(r_{in})$ and the function $g(y)$ is related to stresses. The explicit expressions for $E_\theta(r)$ for some special stress states are given below; otherwise the integral on the right-hand side of Eq. (24) can be numerically evaluated.

For a solid disk of uniform thickness and a constant hoop stress in it, substitution for stresses from Eq. (15) into Eq. (22) gives the required variation of the elastic modulus in the disk as

$$E_\theta(r) = E_{ou} \left(\frac{r}{r_{ou}} \right)^{\frac{\alpha-1}{\alpha(1-\nu_{\theta r})}} \left(\frac{(1-\nu_{\theta r})(3P+1) + \nu_{\theta r} r^2 / r_{ou}^2}{3P(1-\nu_{\theta r}) + 1} \right)^{\frac{1+\nu_{\theta r}\alpha(2-3\nu_{\theta r})}{2\nu_{\theta r}\alpha(1-\nu_{\theta r})}}, \quad (25)$$

where $E_{ou} = E_\theta(r_{ou})$ and $P = \frac{\bar{\sigma}_{rr}^{ou}}{\rho\omega^2 r_{ou}^2}$ is a non-dimensional number. For $\bar{\sigma}_{rr}^{ou} = 0$, we get $P = 0$ and the expression (25) for the elastic modulus becomes

$$E_\theta(r) = E_{ou} \left(\frac{r}{r_{ou}} \right)^{\frac{\alpha-1}{\alpha(1-\nu_{\theta r})}} \left(1 - \nu_{\theta r} + \nu_{\theta r} \frac{r^2}{r_{ou}^2} \right)^{\frac{1+\nu_{\theta r}\alpha(2-3\nu_{\theta r})}{2\nu_{\theta r}\alpha(1-\nu_{\theta r})}}. \quad (26)$$

Thus the required variation of E_θ in the radial direction is independent of the angular speed of the disk.

For the in-plane shear stress to be constant throughout a solid disk of uniform thickness, substitution for the radial and the hoop stresses from Eq. (20) into Eq. (24) and the assumption $\bar{\sigma}_{rr}^{ou} \neq 0$ yields

$$E_\theta(r) = E_{ou} \left(\frac{r}{r_{ou}} \right)^{\frac{\alpha-1}{\alpha(1-\nu_{\theta r})}} \left(1 + \frac{\rho\omega^2 r_{ou}^2}{2\bar{\sigma}_{rr}^{ou}} (1 - r^2 / r_{ou}^2) \right). \quad (27)$$

Setting $\alpha = 1$ in Eq. (27), we find that $E_\theta(r)$ for an isotropic material is the same as that given in Ref. [16], and is independent of Poisson's ratio.

For the radial stress to be a non-zero constant D_0 in a solid disk of uniform thickness, substitution for the radial and the hoop stresses from Eq. (21) into Eq. (24) gives

$$E_\theta(r) = E_{ou} \left(\frac{r}{r_{ou}} \right)^{\frac{\alpha-1}{\alpha(1-\nu_{\theta r})}} \left(\frac{Q(\nu_{\theta r} - 1) - r^2 / r_{ou}^2}{Q(\nu_{\theta r} - 1) - 1} \right)^{\frac{1+\alpha(2-2\nu_{\theta r}-\nu_{\theta r}^2)}{2\alpha(1-\nu_{\theta r})}}, \quad (28)$$

where $Q = \frac{D_0}{\rho\omega^2 r_{ou}^2}$ is a non-dimensional number.

4.2. Annular fiber-reinforced composite disks with fibers along concentric circles

Substituting for the elastic moduli from Eq. (8) and the desired stress states from Eqs. (12)–(21) into Eq. (22), we calculate the required variation of the volume fraction of the fiber to have either the hoop stress or the radial stress or the in-plane shear stress uniform throughout the disk.

For example, let us consider three annular disks composed of E-glass/epoxy having the outer radius $r_{ou} = 100$ mm and the inner radius $r_{in} = 20$ mm, 40 mm, and 60 mm. The elastic moduli are

$$E_f = 72.3 \text{ GPa}, \quad \nu_f = 0.22, \quad E_m = 3.5 \text{ GPa}, \quad \nu_m = 0.33.$$

Substituting for stresses from Eqs. (12) and (8) into Eq. (22) and taking $n = 0$ for the disk of uniform thickness and $\zeta_f(r_{in}) = 0.2$, the required variation of the volume fraction of fibers is plotted in Fig. 3a; the variations of the corresponding elastic moduli are shown in Fig. 3b–d. It is noticed from Fig. 3a that, for $r_{in}/r_{ou} = 0.4$ and 0.6, the volume fraction of fibers is a monotonically increasing function of the radius r in order to achieve a

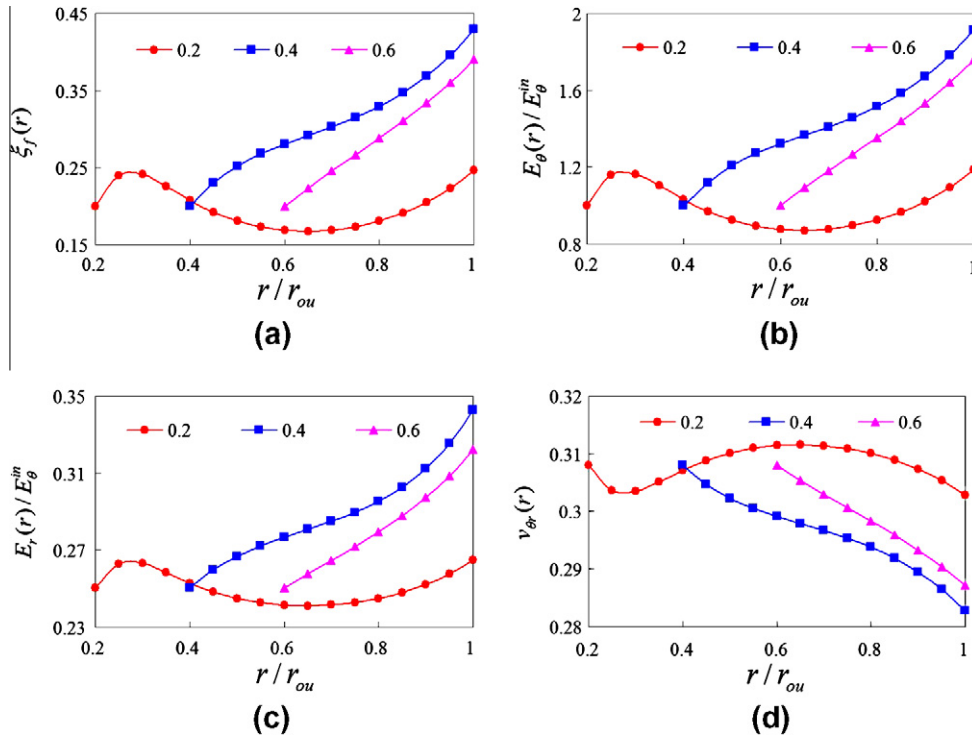


Fig. 3. For a constant hoop stress throughout the disks with $r_{in}/r_{ou} = 0.2, 0.4$ and 0.6 , the required variation with the radius of (a) the volume fraction of fibers, (b) elastic modulus E_θ , (c) elastic modulus E_r , and (d) Poisson's ratio ν_θ .

constant hoop stress throughout the disk. However, for $r_{in}/r_{ou} = 0.2$, the required volume fraction of the fibers at first increases with r , has the maximum value at $r/r_{ou} = 0.28$ and the minimum value at $r/r_{ou} = 0.65$. The variations of the elastic moduli with

the radius r are similar to those of the fiber volume fraction. We note that the volume fraction of fibers varies between 0.16 and 0.25, 0.2 and 0.43 and 0.2 and 0.4 for the three disks studied. One cannot quickly assess the effect of the radial variation in the

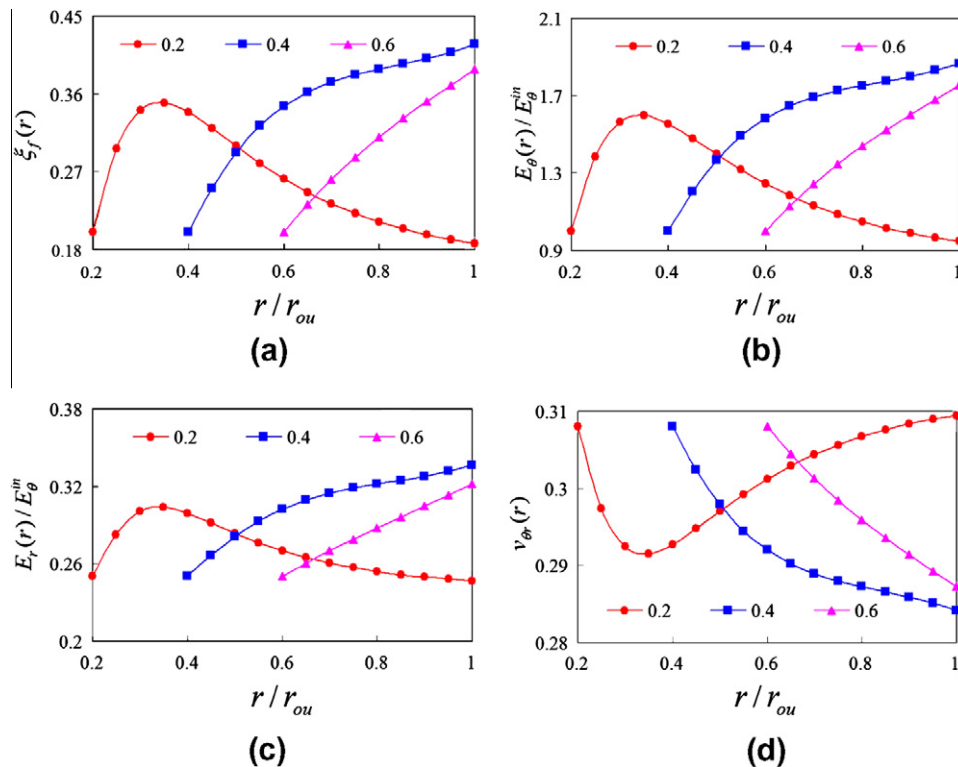


Fig. 4. For constant in-plane shear stress throughout the disks with $r_{in}/r_{ou} = 0.2, 0.4$ and 0.6 , the required variation with the radius of (a) the volume fraction of fiber, (b) elastic modulus E_θ , (c) elastic modulus E_r , and (d) Poisson's ratio ν_θ .

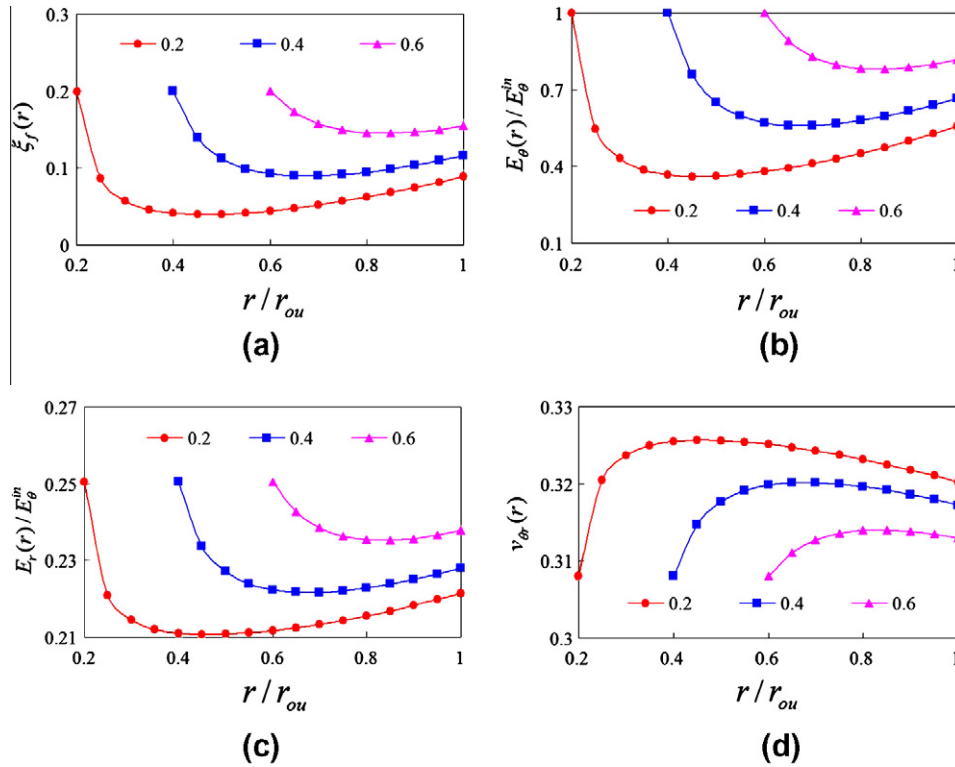


Fig. 5. For a constant radial stress throughout the disks with $r_{in}/r_{ou} = 0.2, 0.4$ and 0.6 , the required variation with the radius of (a) the volume fraction of fiber, (b) elastic modulus E_{θ} , (c) elastic modulus E_r , and (d) Poisson's ratio ν_{θ} .

mass density induced by the change in the volume fraction of fibers on the computed radial variation of the elastic moduli without iteratively solving this problem.

Substituting for stresses from Eqs. (18) and (8) into Eq. (22), the required variations of the elastic moduli with r to attain a constant in-plane shear stress is exhibited in Fig. 4. We note from Fig. 4 that the elastic moduli have the maximum and Poisson's ratio the minimum value at points in the interior of the disk for $r_{in}/r_{ou} = 0.2$.

The variations of the elastic moduli with the radius r are similar for disks with $r_{in}/r_{ou} = 0.4$ and 0.6 but these noticeably differ from those for the disk with $r_{in}/r_{ou} = 0.2$. Thus the ratio r_{in}/r_{ou} of the disk significantly affects the qualitative variation of the elastic moduli with r .

Substituting for stresses from Eqs. (21) and (8) into Eq. (22), the required variations of the elastic moduli to attain a constant radial stress in a disk are found, and these are shown in Fig. 5. It is

observed that the variations of the elastic moduli with the radius are similar for the three disks with $r_{in}/r_{ou} = 0.2, 0.4$ and 0.6 .

We now investigate the effect of the thickness variation on material tailoring. When the disk thickness is either uniform ($n = 0$) or inversely proportional to r ($n = 1$), the required variation of the volume fraction of fibers to achieve the desired stress field is shown in Fig. 6. Curves labeled '0-' (or '1-') represent results for $n = 0$ (or 1) and the second number '0.2' (or '0.6') following 0 and 1 denotes the ratio r_{in}/r_{ou} . It is found that the variation of the thickness has significant effect on the required variation of the volume fraction of fibers to attain the constant hoop stress and the constant in-plane shear stress within the disk having $r_{in}/r_{ou} = 0.2$. However, there is very little influence of the thickness variation on the volume fraction of fibers for the disk with $r_{in}/r_{ou} = 0.6$.

For two different values of the volume fraction of fibers on the innermost surface of a disk, the computed required variations of

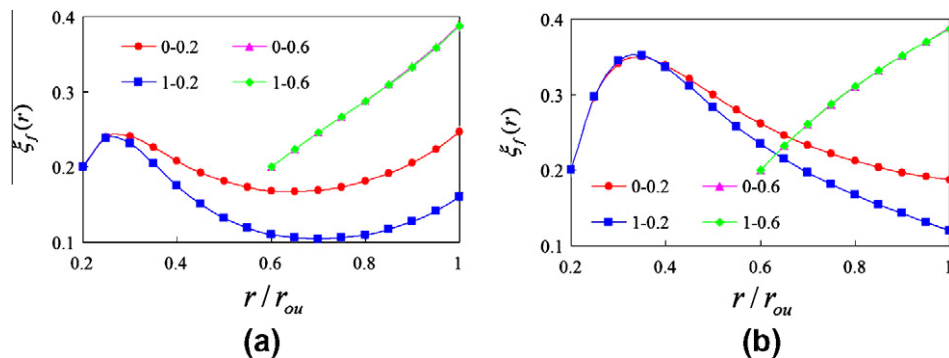


Fig. 6. For disks with $r_{in}/r_{ou} = 0.2$ and 0.6 , and either uniform or non-uniform thickness, the required variation with the radius of the volume fraction of fibers for (a) a constant hoop stress, (b) a constant in-plane shear stress throughout the disk.

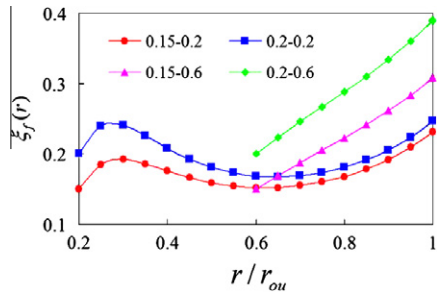


Fig. 7. The required variation with the radius of the volume fraction of fibers to achieve a constant hoop stress in two disks with different values of the volume fraction of fiber on their inner surfaces.

the volume fraction of fibers to achieve the same constant hoop stress are exhibited in Fig. 7. Curves labeled ‘0.15-’ (or ‘0.2-’) represent results for $\xi_f(r_{in}) = 0.15$ (or 0.2) and the second number ‘0.2’ (or ‘0.6’) following 0.15 and 0.2 denotes the ratio r_{in}/r_{ou} . It is seen that different values of $\xi_f(r_{in})$ can give the same stress field within a disk evincing thereby that the inverse problem does not have a unique solution. However, the corresponding displacement fields will be different since stress fields are not sensitive to the precise values of the elastic moduli, e.g., the axial stress in a cylindrical bar of cross-section A and loaded by an axial force, P , equals P/A irrespective of the material of the bar.

4.3. Annular fiber-reinforced composite disks with fibers aligned along helices

Substituting for the elastic constants from Eq. (9) and the desired stress states from Eqs. (12)–(21) into Eq. (22), we can find the required variation of the fiber orientation angle with the radius to attain either a constant hoop stress, or a constant radial stress or a constant in-plane shear stress in the disk.

For example, consider three annular disks composed of T300/934 (graphite/epoxy) with the volume fraction of fibers equal to 0.65 and

$$E_1 = 131 \text{ GPa}, E_2 = 10.3 \text{ GPa}, G_{12} = 6.9 \text{ GPa}, \nu_{12} = 0.22.$$

Substituting for the elastic moduli from Eq. (9) and for stresses from Eqs. (12) and (21), respectively, into Eq. (22) and setting $n = 0$ for the disk of uniform thickness, the required variation of the fiber angle for the condition $\beta(r_{in}) = \pi/4$ is shown in Figs. 8 and 9. Comparing results plotted in Figs. 3–5 with those exhibited in Figs. 8 and 9, it is found that there are different ways to attain the same desired stress state, for example, by either changing the volume fraction of fibers along concentric circles or by varying the orientation of fibers in the radial direction. However, these two material tailoring techniques give different variations with r of the corresponding hoop and the radial elastic moduli. For fibers aligned along concentric circles, the hoop and the radial elastic moduli increase or decrease simultaneously with r . However, when the orientation of fibers in the radial direction is varied, the corresponding hoop and the radial elastic moduli increase and decrease, respectively, with an increase in the radius r .

5. Conclusions

We have investigated the material tailoring problem for a rotating disk composed of a radially inhomogeneous material to attain either a constant hoop stress, or a constant radial stress or a constant in-plane shear stress throughout the disk. For a solid disk made of a material with the elastic moduli proportional to each other, an analytical expression is given for the required variation of the hoop modulus with the radius to attain a desired state of stress. For fiber-reinforced composites, the hoop and the radial elastic moduli increase or decrease simultaneously when we change the volume fraction of fibers that are arranged along concentric circles. However, when the fiber orientation angle is

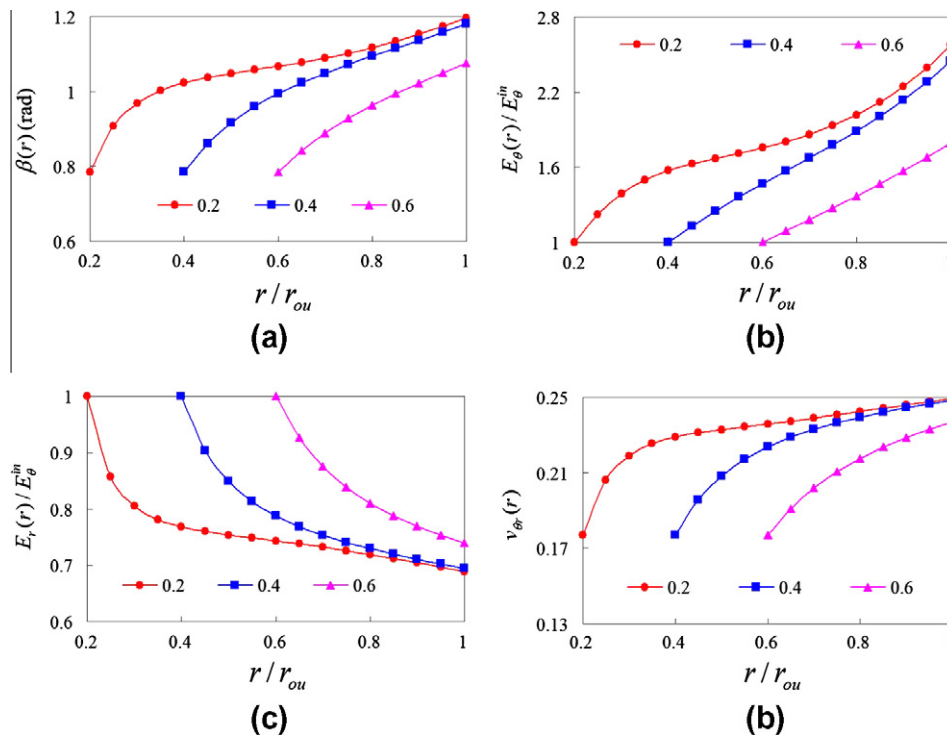


Fig. 8. For a constant hoop stress in disks with $r_{in}/r_{ou} = 0.2, 0.4$ and 0.6 , the required variations with the radius of (a) the orientation of fibers, (b) elastic modulus E_θ , (c) elastic modulus E_r , and (d) Poisson's ratio $\nu_{\theta r}$.

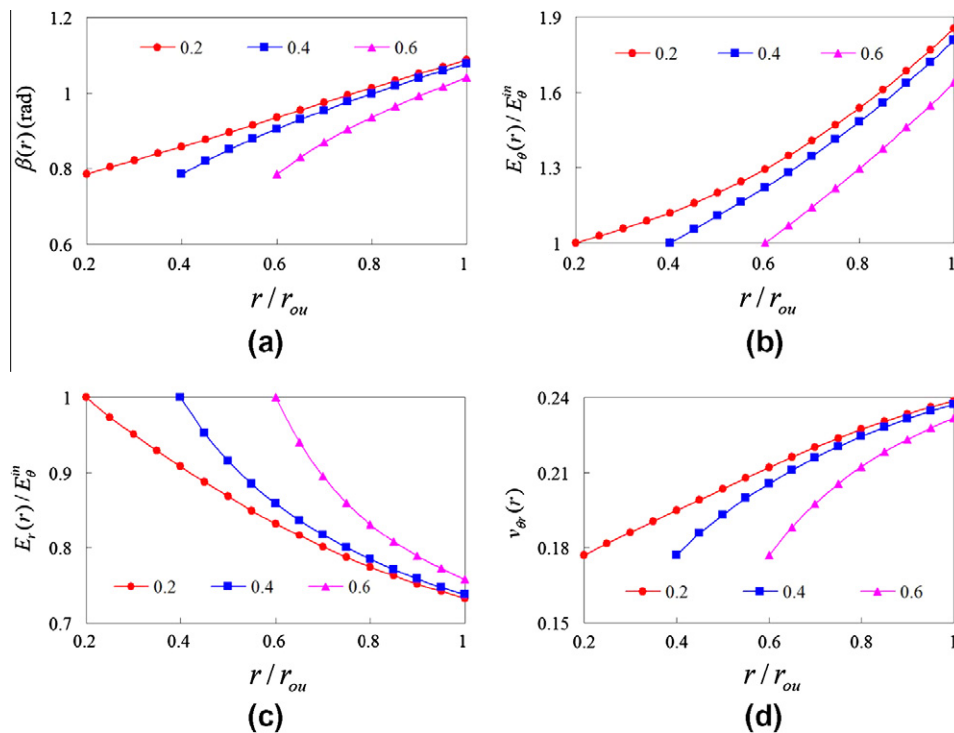


Fig. 9. For a constant radial stress throughout the disks with $r_{in}/r_{ou} = 0.2, 0.4$ and 0.6 , the required variation with the radius of (a) the orientation of fibers, (b) elastic modulus E_{θ} , (c) elastic modulus E_r , and (d) Poisson's ratio ν_{θ} .

varied with the radius, the hoop elastic modulus increases with r but the radial elastic modulus decreases with r . Other constraints, e.g., minimizing the weight, can help decide whether to achieve material tailoring with fibers arranged in concentric circles or in helices. For a very thick rotating disk (e.g., $r_{in}/r_{ou} = 0.2$) the influence of the non-uniform thickness is evident in the sense that the required radial variation of the volume fraction of fibers is distinctly different from that for a moderately thick disk.

The material tailoring techniques presented herein will help structural engineers and material scientists design radially inhomogeneous rotating disks.

Acknowledgments

This work was supported by the Research Fund for the Doctoral Program of Higher Education (No. 20070247029) and the National Natural Science Foundation of China (No. 10872150, 11072177). RCB's work was partially supported by the Office of Naval Research Grant N00014-1-06-0567 to Virginia Polytechnic Institute and State University with Dr. Y.D.S. Rajapakse as the program manager. Views expressed in the paper are those of authors and neither of the funding agencies nor of their Institutions.

References

- [1] Bakare IO, Okieimen FE, Pavithran C, Khalil HPSA, Brahmakumar M. Mechanical and thermal properties of sisal fiber-reinforced rubber seed oil-based polyurethane composites. *Mater Des* 2010;31:4274–80.
- [2] Liu DY, Wang CY, Chen WQ. Free vibration of FGM plates with in-plane material inhomogeneity. *Compos Struct* 2010;92(5):1047–51.
- [3] Aragh BS, Yas MH. Three-dimensional analysis of thermal stresses in four-parameter continuous grading fiber reinforced cylindrical panels. *Int J Mech Sci* 2010;52:1047–63.
- [4] Aragh BS, Yas MH. Three-dimensional free vibration of functionally graded fiber orientation and volume fraction cylindrical panels. *Mater Des* 2010;31:4543–52.
- [5] Kushwaha PK, Kumar R. The studies on performance of epoxy and polyester-based composites reinforced with bamboo and glass fibers. *J Reinf Plast Compos* 2010;29:1952–62.
- [6] Hosseini-Hashemi S, Fadaee M, Es'haghi M. A novel approach for in-plane/out-of-plane frequency analysis of functionally graded circular/annular plates. *Int J Mech Sci* 2010;52:1025–35.
- [7] Vel SS. Exact elasticity solution for the vibration of functionally graded anisotropic cylindrical shells. *Compos Struct* 2010;92:2712–27.
- [8] Malekzadeh P, Beni AA. Free vibration of functionally graded arbitrary straight-sided quadrilateral plates in thermal environment. *Compos Struct* 2010;92:2758–67.
- [9] Hosseini SM, Shahabian F. Reliability of stress field in Al–Al₂O₃ functionally graded thick hollow cylinder subjected to sudden unloading, considering uncertain mechanical properties. *Mater Des* 2010;31:3748–60.
- [10] Kang YA, Li XF. Large deflections of a non-linear cantilever functionally graded beam. *J Reinf Plast Compos* 2010;29:1761–74.
- [11] Leissa AW, Vagins M. The design of orthotropic materials for stress optimization. *Int J Solids Struct* 1978;14:517–26.
- [12] Pardoen GC, Nudenberg RD, Swartout BE. Achieving desirable stress states in thick rim rotating disks. *Int J Mech Sci* 1981;23:367–82.
- [13] Danfelt EL, Hewes SA, Chou TW. Optimization of composite flywheel design. *Int J Mech Sci* 1977;19:69–78.
- [14] Adali S, Verijenko VE, Chevallereau B. Design optimization of composite rotating discs under multiple loads. *AIAA J* 1998:890–6.
- [15] Gowayed Y, Abel-Hady F, Flowers GT, Trudell JJ. Optimal design of multi-direction composite flywheel rotors. *Polym Compos* 2002;23:433–41.
- [16] Jain R, Ramachandra K, Simha KRY. Rotating anisotropic disc of uniform strength. *Int J Mech Sci* 1999;41:639–48.
- [17] Güven U, Çelik A, Baykara C. On transverse vibrations of functionally graded polar orthotropic rotating solid disk with variable thickness and constant radial stress. *J Reinf Plast Compos* 2004;23:1279–84.
- [18] Fabien BC. The influence of failure criteria on the design optimization of stacked-ply composite flywheels. *Struct Multidisc Optim* 2007;33:507–17.
- [19] Cho HK, Rowlands RE. Optimizing fiber direction in perforated orthotropic media to reduce stress concentration. *J Compos Mater* 2009;43:1177–98.
- [20] Tanaka K, Tanaka Y, Enomoto K, Poterasu VF, Sugano Y. Design of thermoelastic materials using direct sensitivity and optimization methods: reduction of thermal stresses in functionally gradient materials. *Comput Methods Appl Mech Eng* 1993;106:271–84.
- [21] Tanaka K, Tanaka Y, Watanabe H, Poterasu VF, Sugano Y. An improved solution to thermoelastic material design in functionally gradient materials: scheme to reduce thermal stresses. *Comput Methods Appl Mech Eng* 1993;109:377–89.
- [22] Tanaka K, Watanabe H, Sugano Y, Poterasu VF. A multicriteria material tailoring of a hollow cylinder in functionally gradient materials: scheme to global reduction of thermoelastic stresses. *Comput Methods Appl Mech Eng* 1996;135:369–80.
- [23] Batra RC, Jin J. Natural frequencies of a functionally graded rectangular plate. *J Sound Vib* 2005;282:509–16.
- [24] Qian LF, Batra RC. Design of bidirectional functionally graded plate for optimal natural frequencies. *J Sound Vib* 2005;280:415–24.

- [25] Goupee AJ, Vel SS. Two-dimensional optimization of material composition of functionally graded materials using meshless analyses and a genetic algorithm. *Comput Methods Appl Mech Eng* 2006;195:5926–48.
- [26] Goupee AJ, Vel SS. Multi-objective optimization of functionally graded materials with temperature-dependent material properties. *Mater Des* 2007;28:1861–79.
- [27] Batra RC. Optimal design of functionally graded incompressible linear elastic cylinders and spheres. *AIAA J* 2008;46:2050–7.
- [28] Nie GJ, Batra RC. Exact solutions and material tailoring for functionally graded hollow circular cylinders. *J Elasticity* 2010;99:179–201.
- [29] Nie GJ, Batra RC. Material tailoring and analysis of functionally graded isotropic and incompressible linear elastic hollow cylinders. *Compos Struct* 2010;92:265–74.
- [30] Nie GJ, Batra RC. Stress analysis and material tailoring in isotropic linear thermoelastic incompressible functionally graded rotating disks of variable thickness. *Compos Struct* 2010;92:720–9.
- [31] Timoshenko SP, Goodier JN. *Theory of elasticity*. 3rd ed. Singapore: McGraw-Hill; 1984.
- [32] Dowling NE. *Mechanical behavior of materials*. Upper Saddle River, New Jersey; 2007.
- [33] Charalambakis N. Homogenization techniques and micromechanics. A survey and perspectives. *Appl Mech Rev* 2010;63 [Art. No. 030803].
- [34] Gibson RF. *Principles of composite material mechanics*. New York: McGraw-Hill; 1994.
- [35] Bert CW, Niedenfuhr FW. Stretching of a polar-orthotropic disk of varying thickness under arbitrary body forces. *AIAA J* 1963;1:1385–90.